

# Computational Modeling in Support of the Magnetic Intervention Concept

D. V. Rose,\* T. C. Genoni, R. E. Clark,  
D. R. Welch, and T. P. Hughes  
*Voss Scientific, LLC*

A. E. Robson, J. D. Sethian, and J. Giuliani, Jr.  
*Naval Research Laboratory*

*HAPL Meeting*  
*Princeton Plasma Physics Laboratory*  
*December 12-13, 2006*

# Outline

1. Description of EMHD model in cylindrical coordinates (based on model of D. Hewett)
2. Direct comparison of explicit PIC simulation to EMHD model
3. EMHD model of R. E. Pechacek magnetic intervention experiment
4. Preliminary EMHD modeling of “chamber-scale” magnetic intervention
5. Next steps...

# 1.) EMHD model implementation based on work of D. Hewett\*

---

- We have implemented a version of D. Hewett's 2D cylindrical ( $r, z$ ) field solver (advancing  $A_\theta$ )
- Model includes “correct” evolution of vacuum magnetic fields
- Field solver implemented within Lsp code framework

\*D. W. Hewett, J. Comp. Phys. **38**, 378 (1980)

# Equation for $A_\theta$

---

$$\frac{\partial A_\theta}{\partial t} - \frac{c^2}{4\pi\sigma} \nabla^2 \vec{A} \Big|_\theta + u_{er} \frac{1}{r} \frac{\partial(rA_\theta)}{\partial r} + u_{ez} \frac{\partial A_\theta}{\partial z} = 0$$

Conductivity is assumed to be a scalar to avoid carrying extra terms

$B_\theta$  can be obtained between ADI passes, but we have not implemented this yet.

In vacuum, this equation reduces to:

$$\nabla^2 \vec{A} \Big|_\theta = 0$$

# Model Constraints:

---

- Most of the computational constraints associated with our previous EMHD solvers also apply here.
- In addition, a “grid-Reynolds” constraint applies, that when combined with the usual diffusion-rate constraint give the following inequality:

$$\left(\frac{c^2}{4\pi}\right)\frac{2\Delta t}{(\Delta x)^2} < \sigma(\text{s}^{-1}) < \frac{2}{\nu \Delta x} \left(\frac{c^2}{4\pi}\right)$$

## 2.) Comparison of explicit EM PIC simulation and EMHD simulation:

- Important benchmark of the EMHD model
- Assess impact of EMHD approximations on magnetic intervention modeling
- Explicit EM PIC uses
  - Inertial macro-particles for both ions and electrons
  - Complete set of Maxwell's equations on finite grid

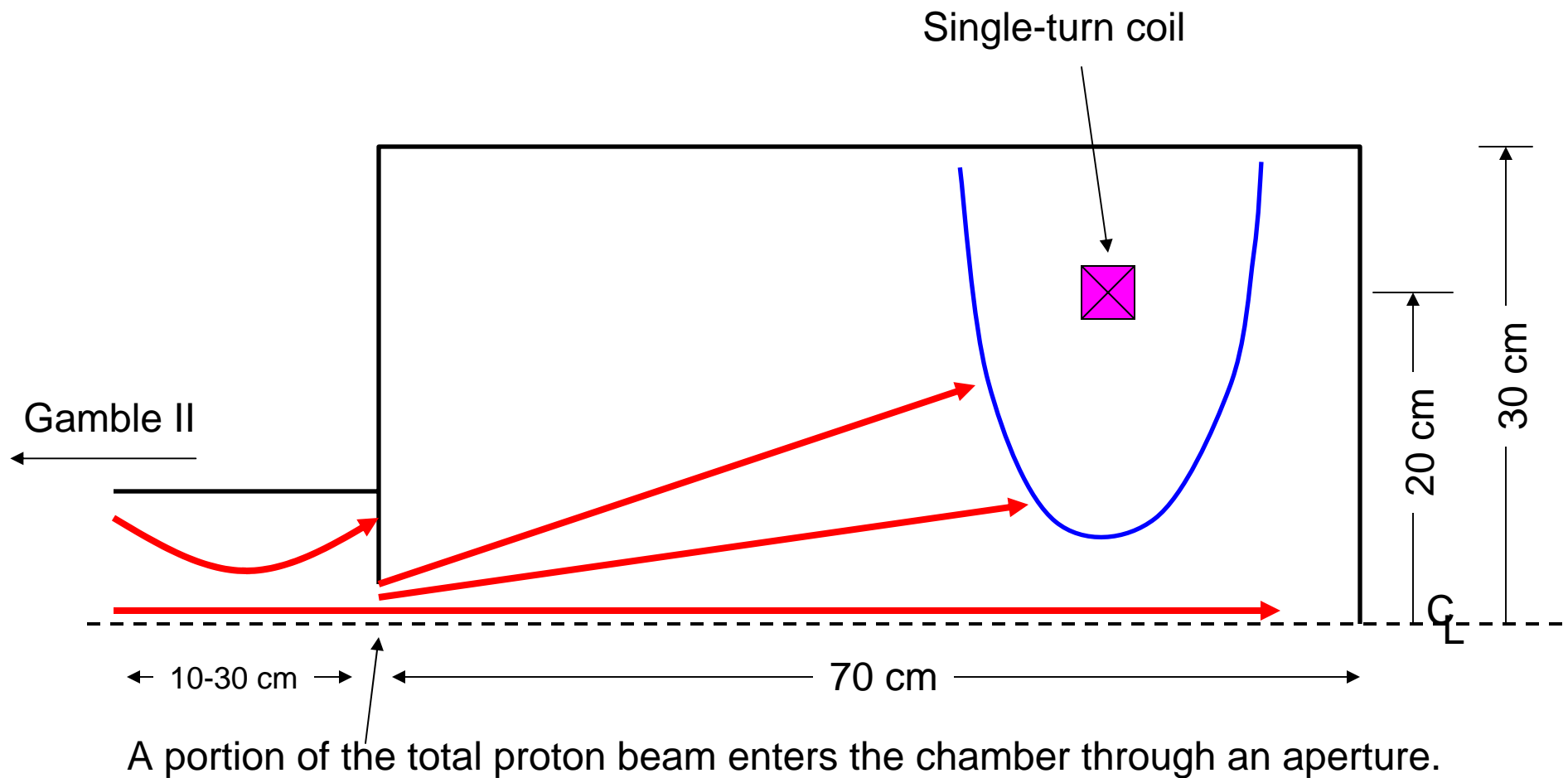
The comparison is carried out using the simulation geometry for the (ill-fated) Gamble II experiment\*:

---

- Explicit simulations for this problem geometry already completed.
- Relatively small-scale simulation problem for the EMHD algorithm (easily satisfying computational constraints for a relatively high conductivity)
- PIC simulations demonstrated diamagnetic penetration of a plasma into an applied magnetic field with a well defined electron sheath formed at the plasma/magnetic-field interface

\*See D. V. Rose, *et. al* presentation, HAPL Meeting, ORNL, March 21, 2006

# Gamble II Experiment: Schematic

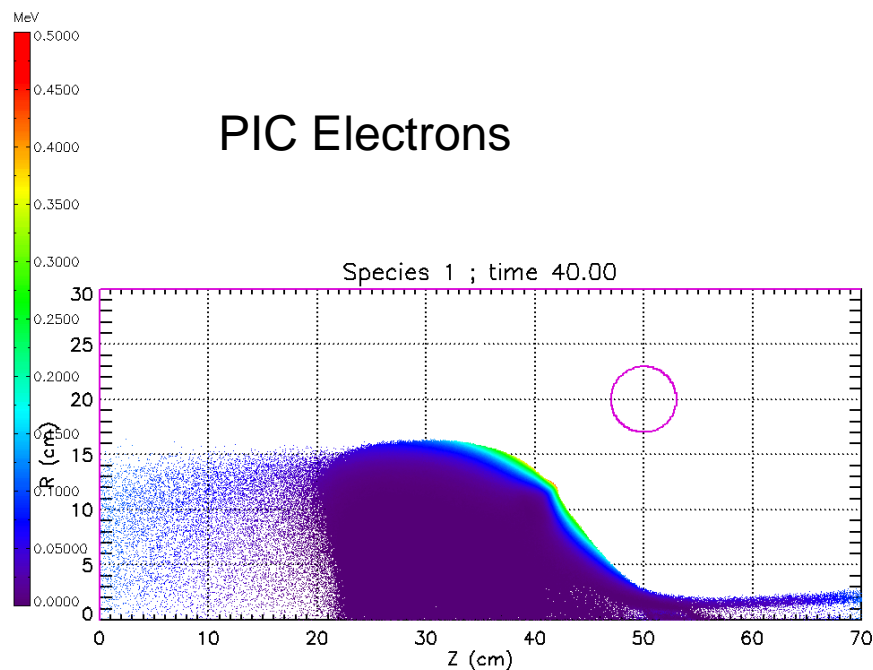




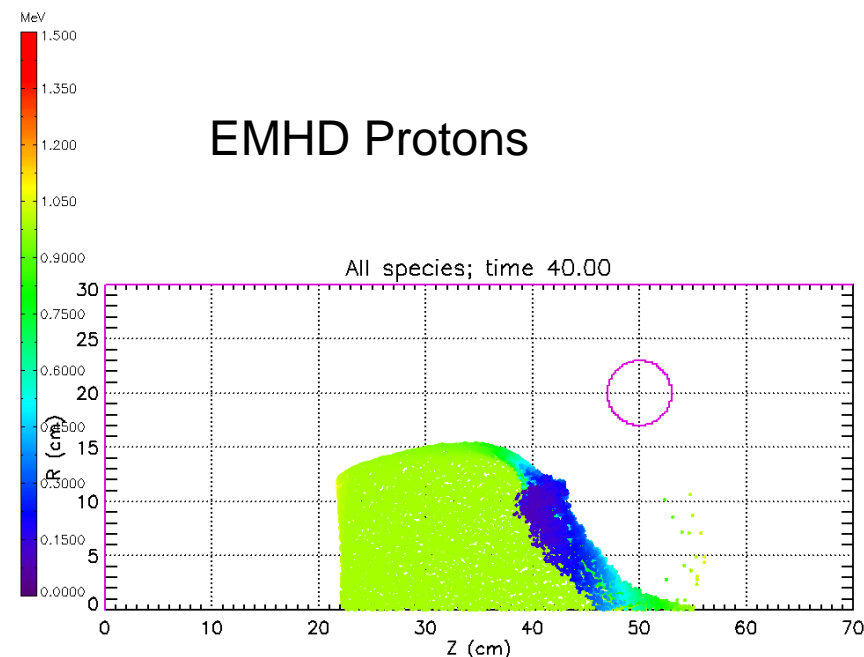
# Comparison: Proton dynamics at the sheath are essentially equivalent at 40 ns.

EMHD sim: ~15,600 particles (protons)  
Explicit PIC sim: ~ 2,000,000 particles  
(1,700,000 electrons, 300,000 protons)

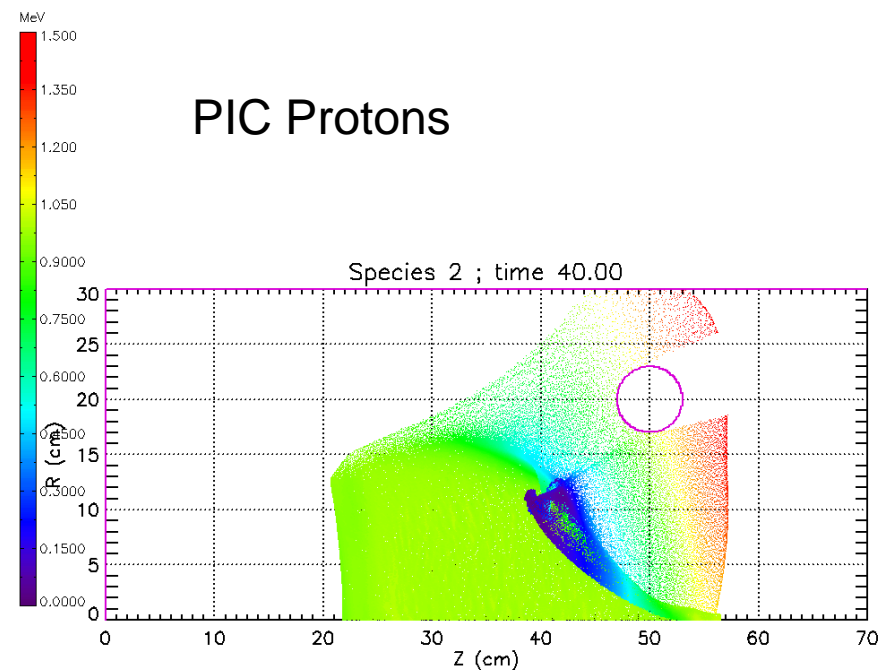
Gamble II MI expt., B=1.6kG, 20 deg, mono-energetic: gamble.isp — Wed Mar 15 14:11:33 20



Gamble II MI expt., B=1.6kG, 20 deg, mono-energetic, no-vacE: gamble.isp — Wed Nov 15 0

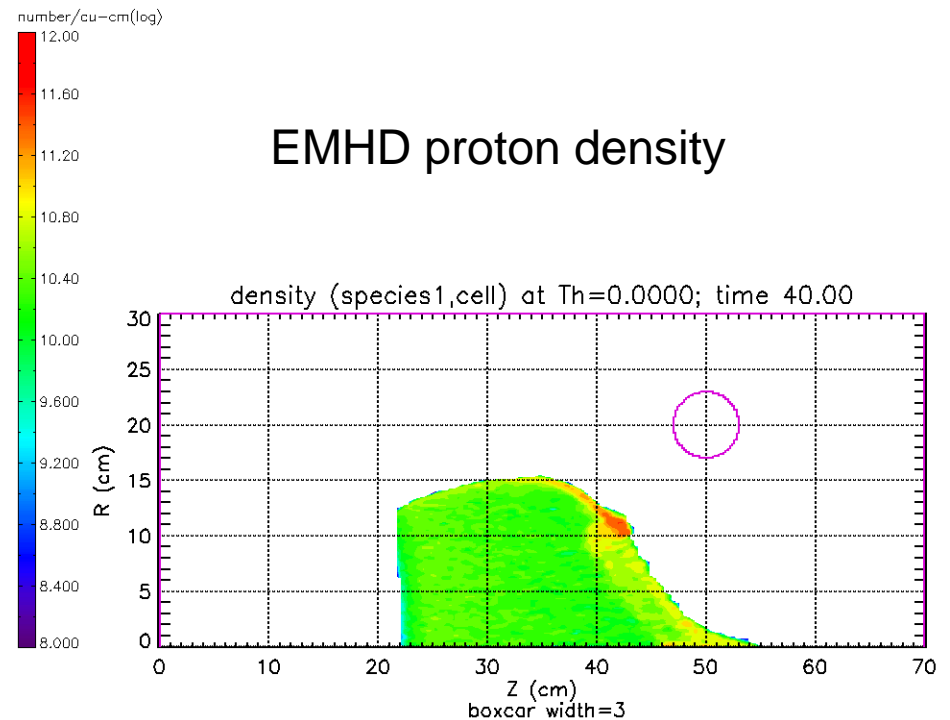
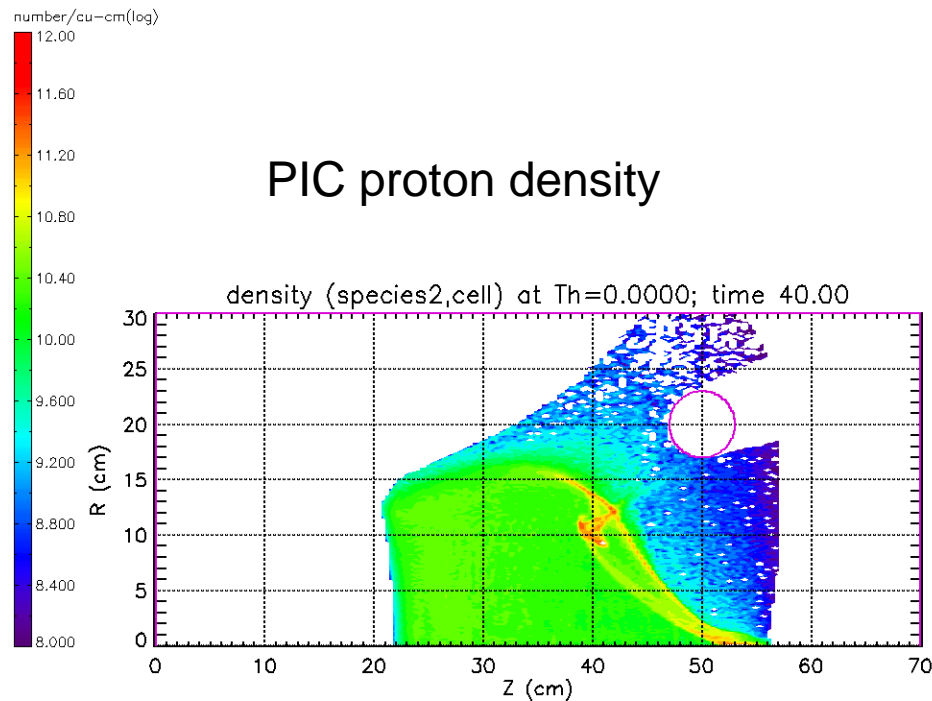


Gamble II MI expt., B=1.6kG, 20 deg, mono-energetic: gamble.isp — Wed Mar 15 14:11:33 20



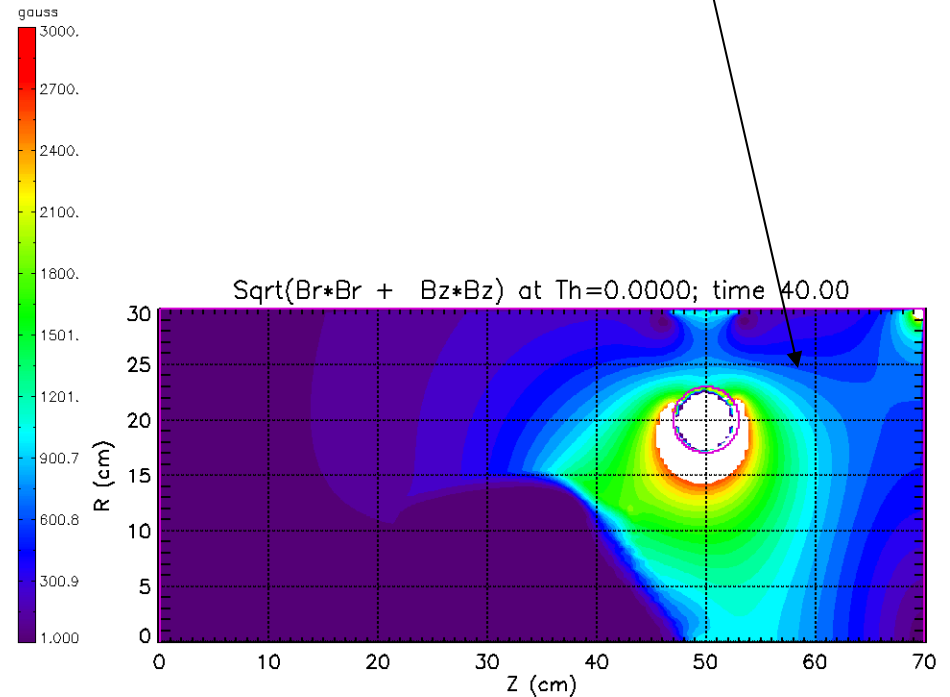
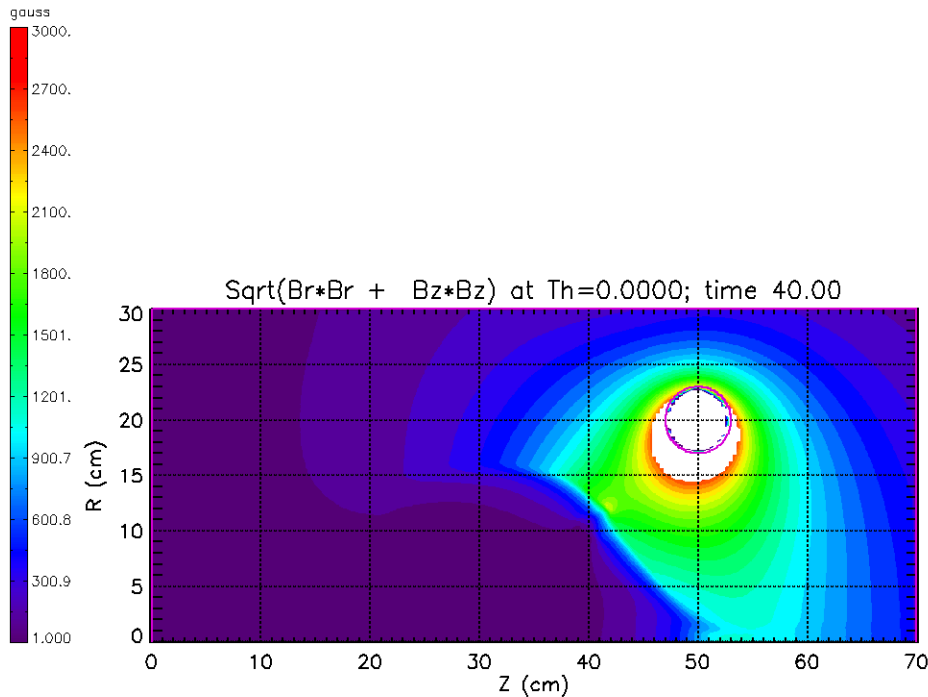
The proton density at 40 ns is remarkable similar: the density pile-up at  $(r,z)=(12,42)$  is even present, although less well resolved in the EMHD simulation.

Gamble II MI expt., B=1.6kG, 20 deg, mono-energetic: gamble.lsp - Wed Mar 15 14:11:33 2000 Gamble II MI expt., B=1.6kG, 20 deg, mono-energetic, no-vacE: gamble.lsp - Wed Nov 15 0



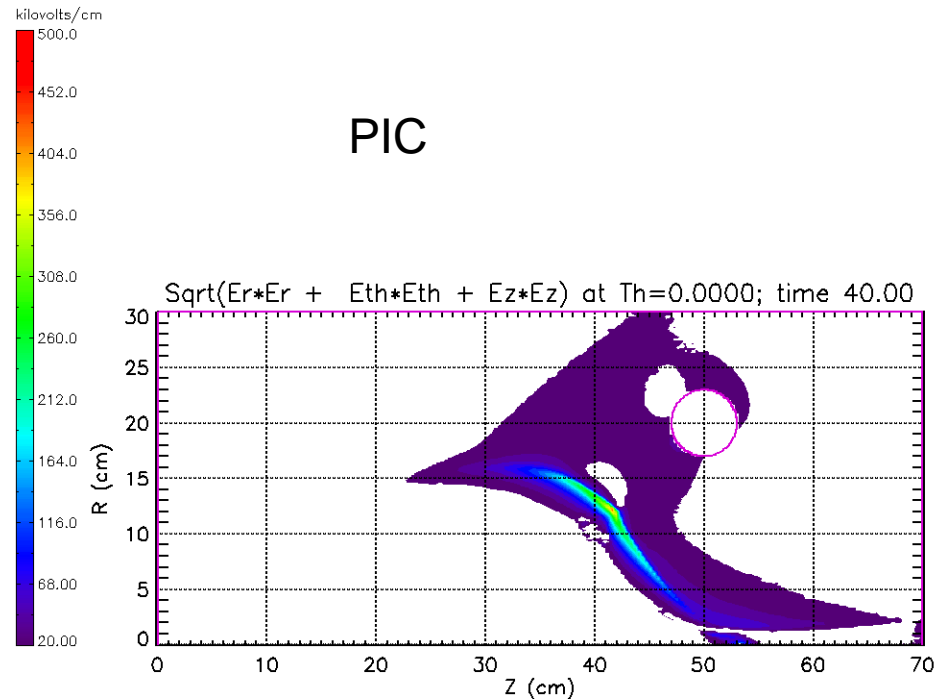
Contours of  $|B|$  in the vicinity of the sheath are in agreement. EMHD solution at large radius and on opposite side of coil is bad.

Gamble II MI expt., B=1.6kG, 20 deg, mono-energetic: gamble.lsp - Wed Mar 15 14:11:33 2000 Gamble II MI expt., B=1.6kG, 20 deg, mono-energetic, no-vacE: gamble.lsp - Wed Nov 15 0 00

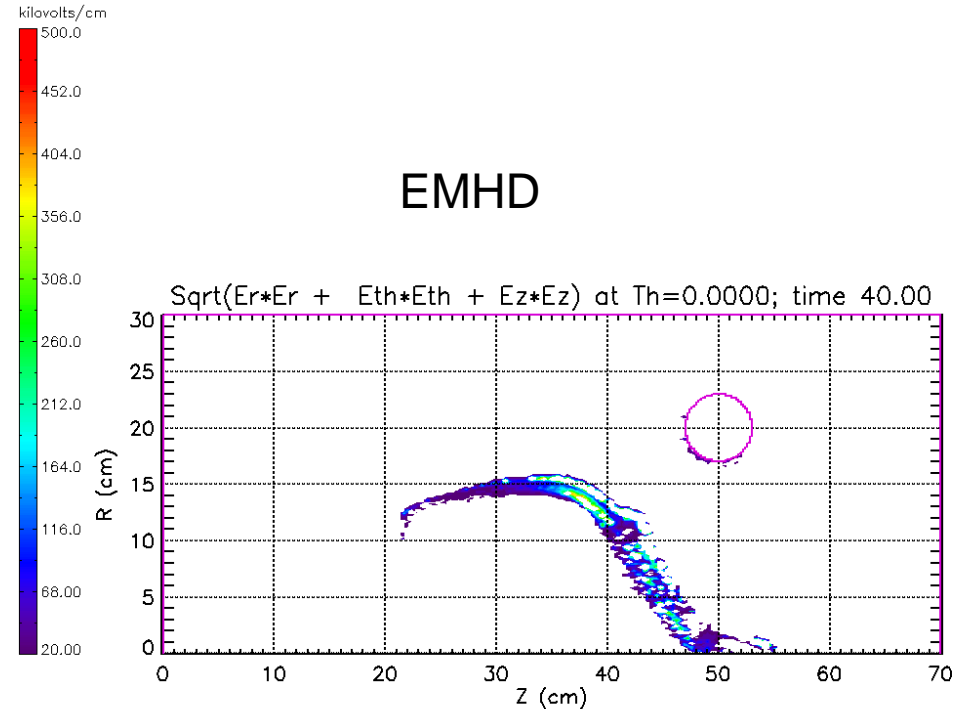


E-fields in vacuum region are huge (up to  $10^4$  kV/cm) and non-physical in the EMHD calculation by 40 ns. PIC shows E-fields confined to thin sheath region only.

Gamble II MI expt., B=1.6kG, 20 deg, mono-energetic: gamble.lsp - Wed Mar 15 14:11:33



Gamble II MI expt., B=1.6kG, 20 deg, mono-energetic, no-vacE: gamble.lsp - Wed Nov 15 0



# 3: Pechacek Experiment Modeling

---

- A two-stage laser system drives a 1-mm scale, solid  $D_2$  pellet forming a plasma.
- The plasma is created inside the void of a cusp magnetic field.
- The adiabatically expanding plasma compresses the cusp field lines.
- Plasma ions escape from the “point” and “ring” cusps in the field geometry.
- Plasma ions are “deflected” away from the chamber walls

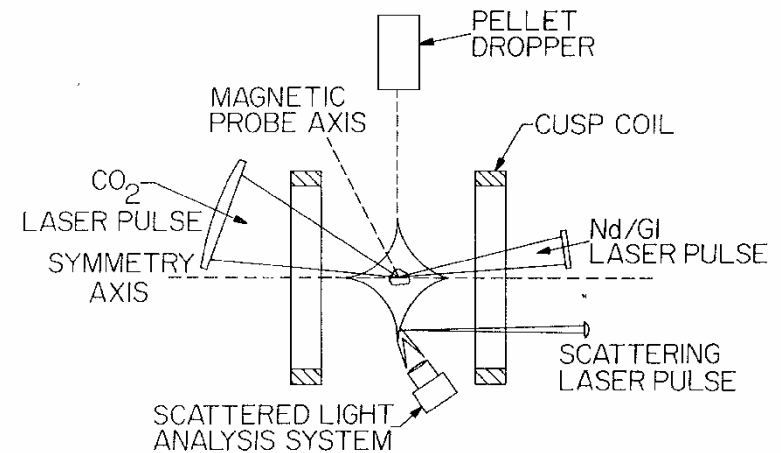
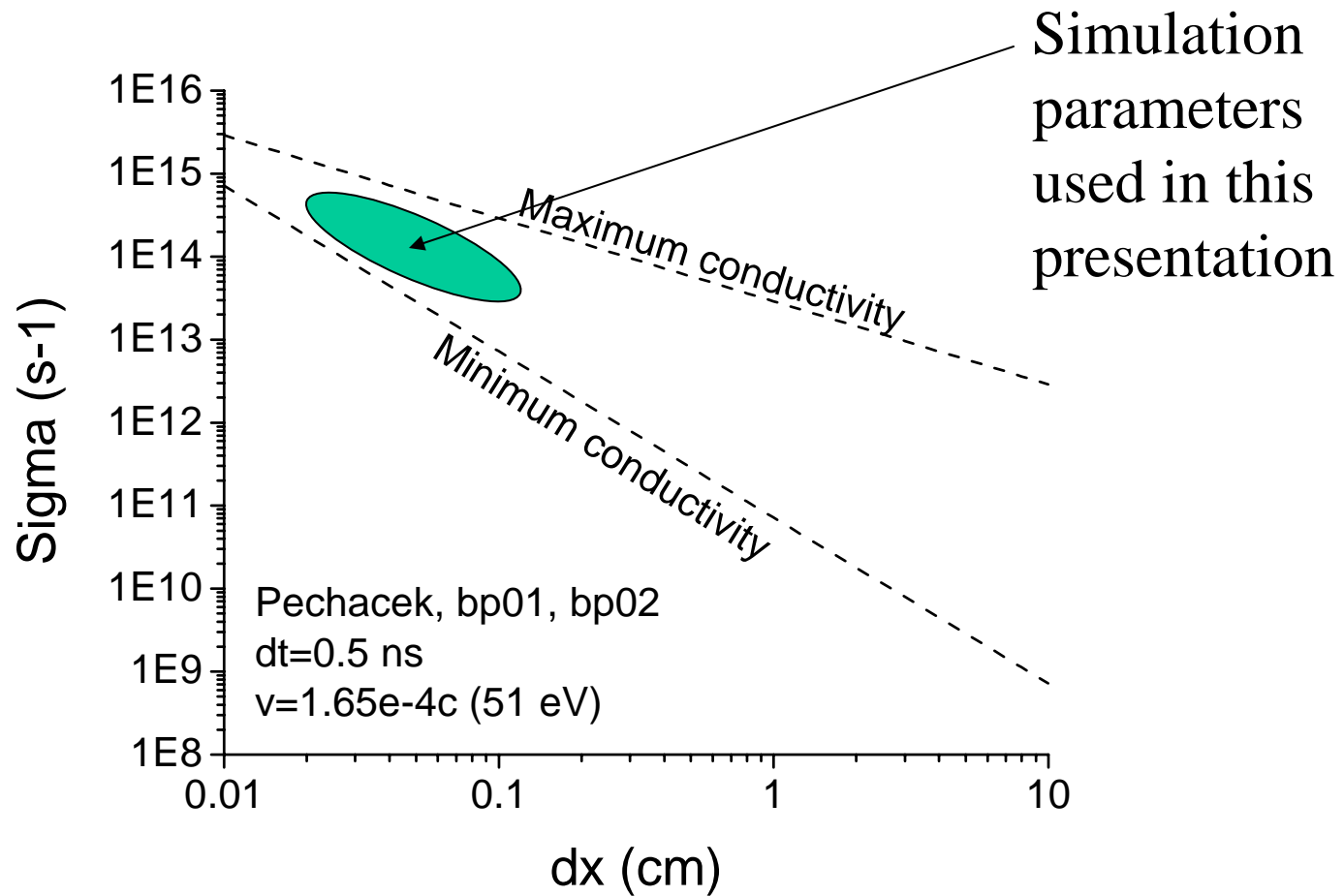


FIG. 1. Schematic diagram of the cusp experiment. The coil diameter is 70 cm. The scattered-light analyzing system and the incident-scattering laser pulse are actually in the same horizontal plane.

\*R. E. Pechacek, *et al.*, Phys. Rev. Lett. **45**, 256 (1980).

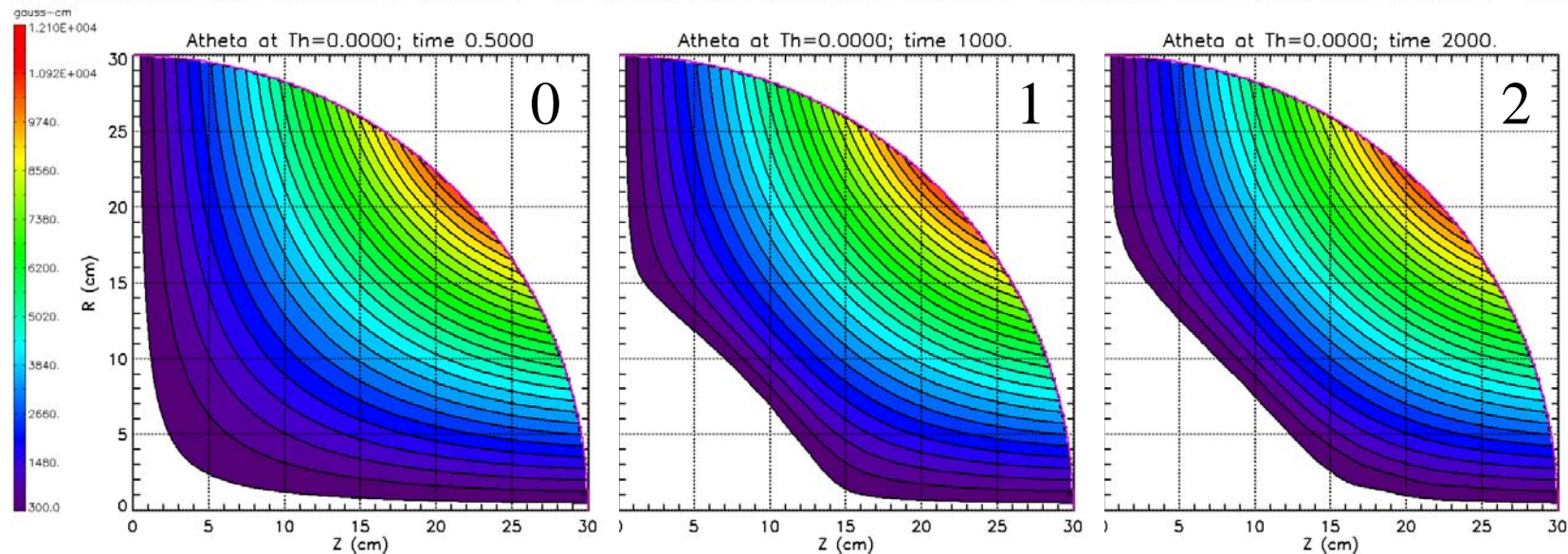
The grid-Reynolds constraints suggests a reasonably wide parameter space for the Pechacek experiment





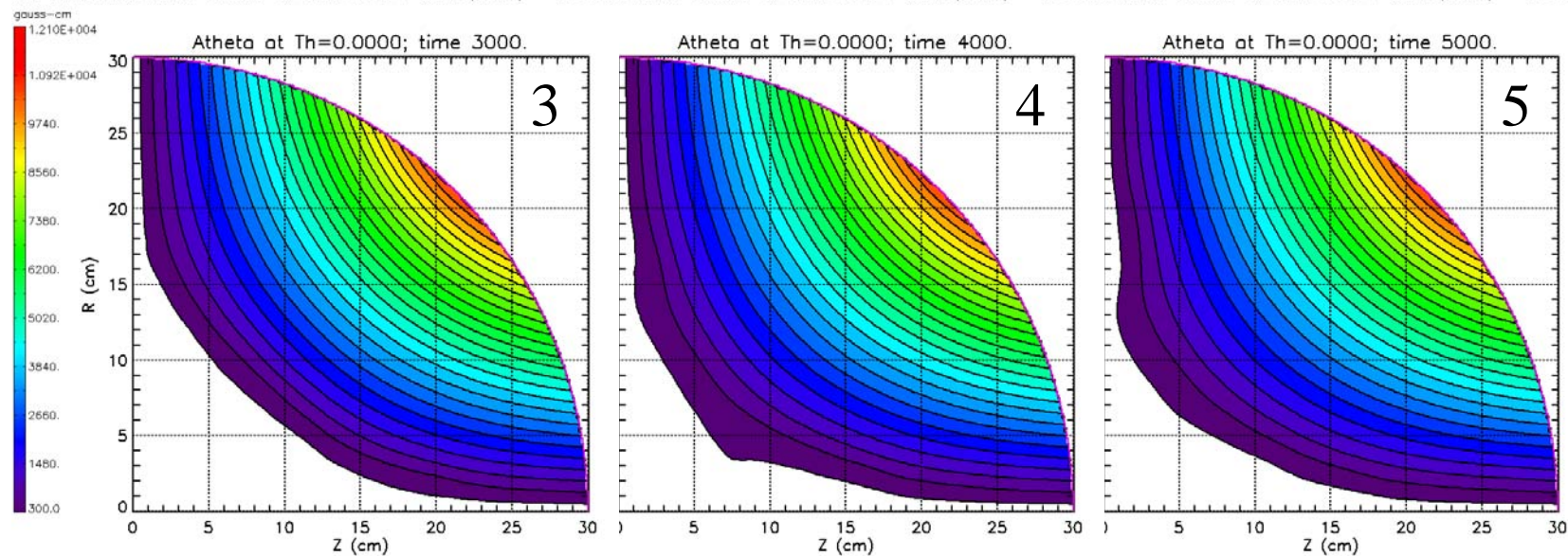
# Magnetic field evolution ( $|A_\theta|$ ):

non-Maxwellian, EMHD, uniform-Q, mono-E, 1 E-iter: bp11.lsp - Sat Dec, EMHD, uniform-Q, mono-E, 1 E-iter: bp11.lsp - Sat Dec, EMHD, uniform-Q, mono-E, 1 E-iter: bp11.lsp - Sat Dec



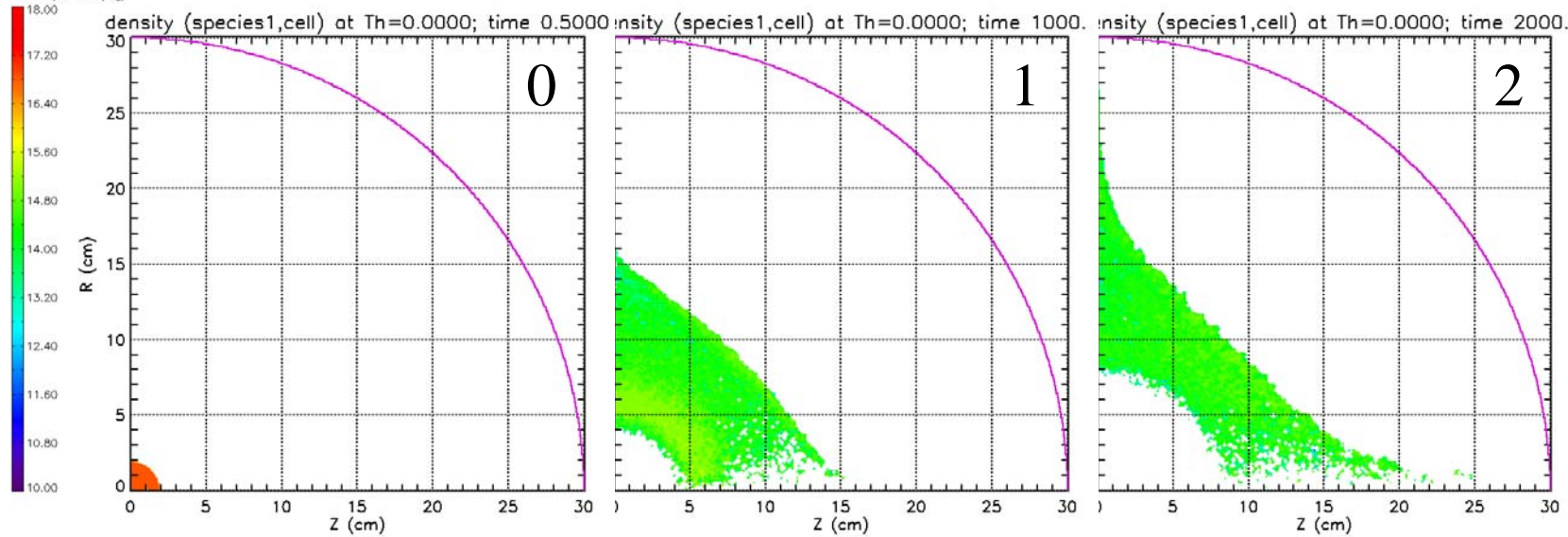
Frames  
at  $n \mu s$   
times

non-Maxwellian, EMHD, uniform-Q, mono-E, 1 E-iter: bp11.lsp - Sat Dec, EMHD, uniform-Q, mono-E, 1 E-iter: bp11.lsp - Sat Dec, EMHD, uniform-Q, mono-E, 1 E-iter: bp11.lsp - Sat Dec



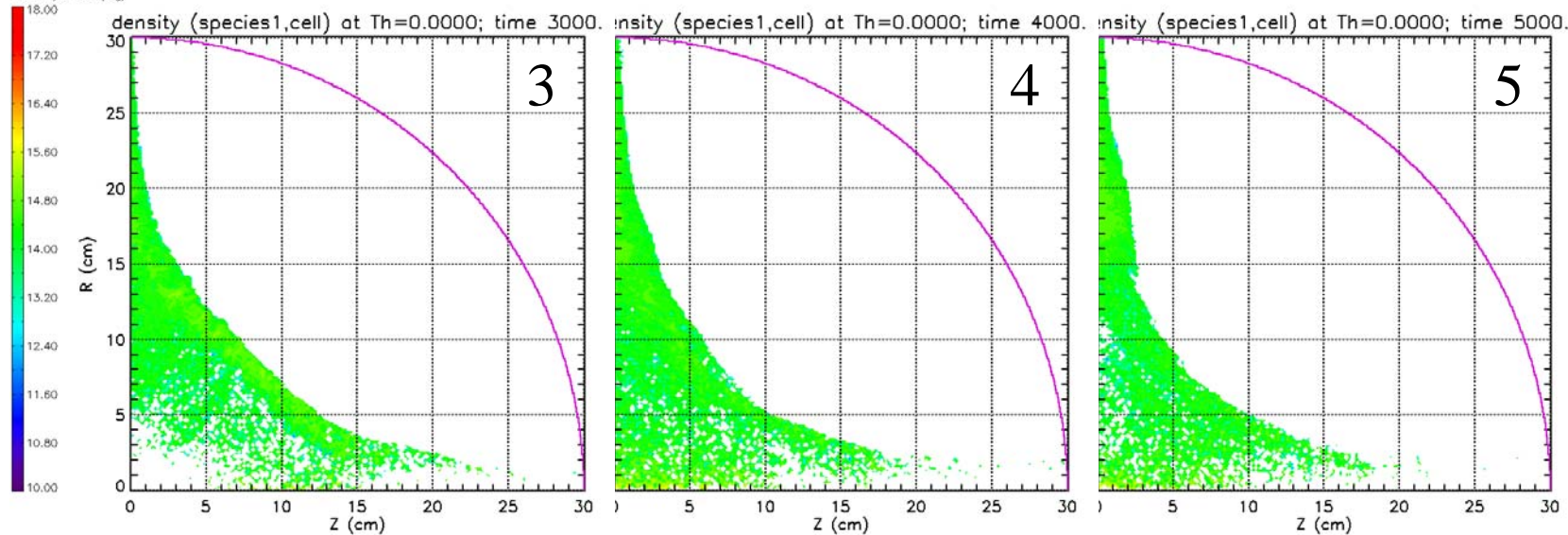
# Ion Density Evolution:

non-Maxwellian, EMHD, uniform-Q, mono-E, 1 E-iter: bp11.lsp - Sat Dec, EMHD, uniform-Q, mono-E, 1 E-iter: bp11.lsp - Sat Dec, EMHD, uniform-Q, mono-E, 1 E-iter: bp11.lsp - Sat Dec



Frames  
at  $n \mu s$   
times

non-Maxwellian, EMHD, uniform-Q, mono-E, 1 E-iter: bp11.lsp - Sat Dec, EMHD, uniform-Q, mono-E, 1 E-iter: bp11.lsp - Sat Dec, EMHD, uniform-Q, mono-E, 1 E-iter: bp11.lsp - Sat Dec





# Status: Pechacek Experiment Modeling

---

- Present modeling is providing the best results to date, and detailed comparisons with the data are very compelling.
- Some problems resolved others remain with the EMHD solver (more work is required).
- Additional developments such as convergence testing and the use of canned, parallelized solvers (e.g. PETSC) are expected to make the algorithm faster.

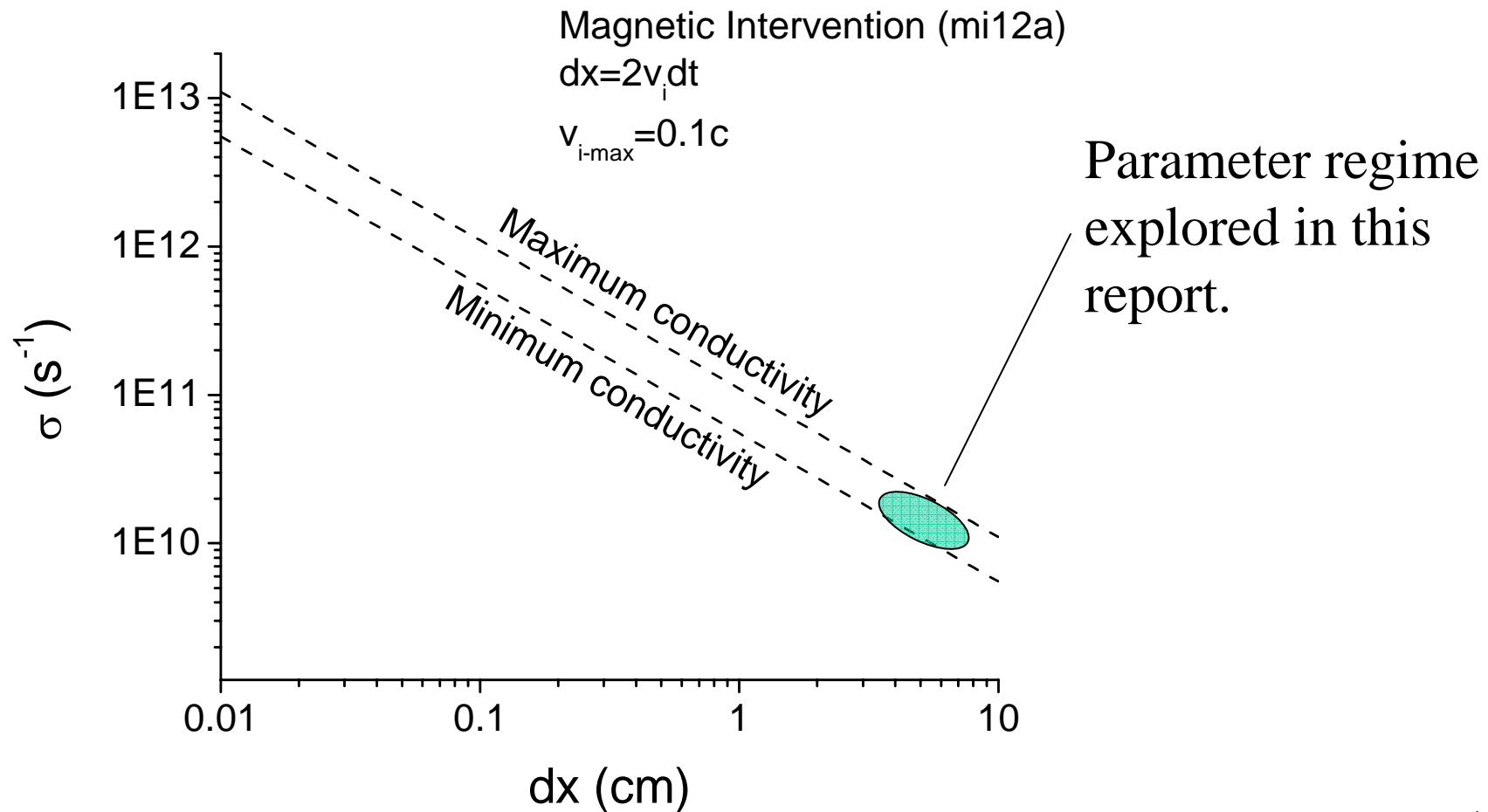
### 3. Chamber-Scale Magnetic Intervention Simulation:

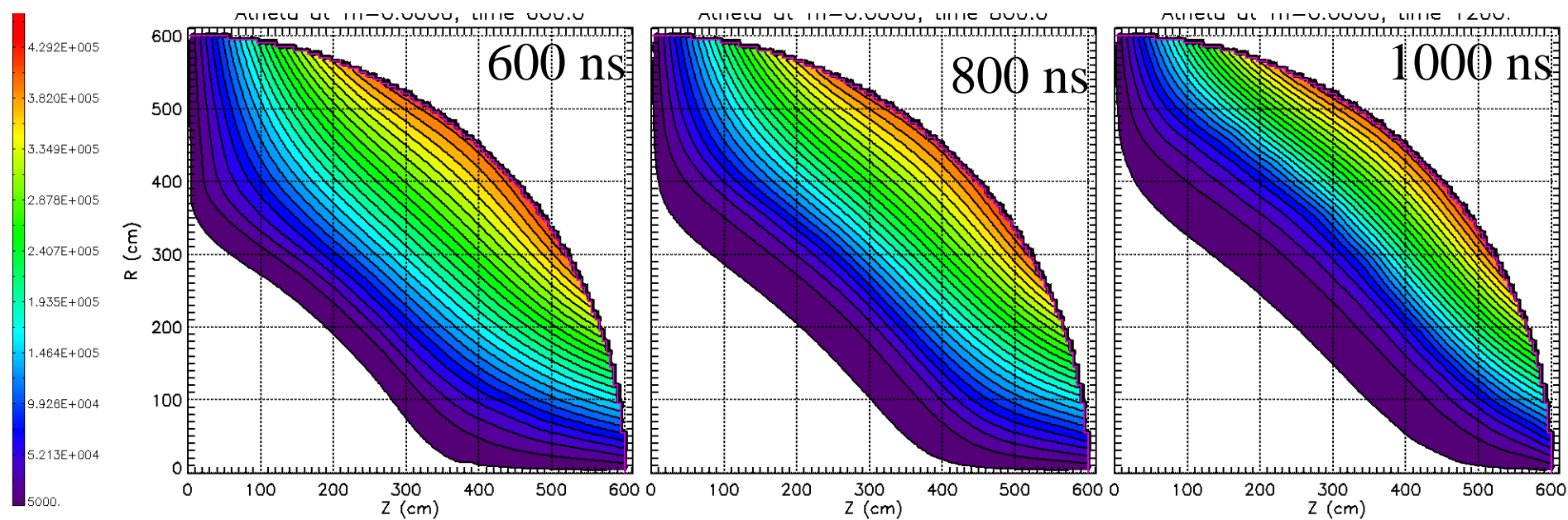
---

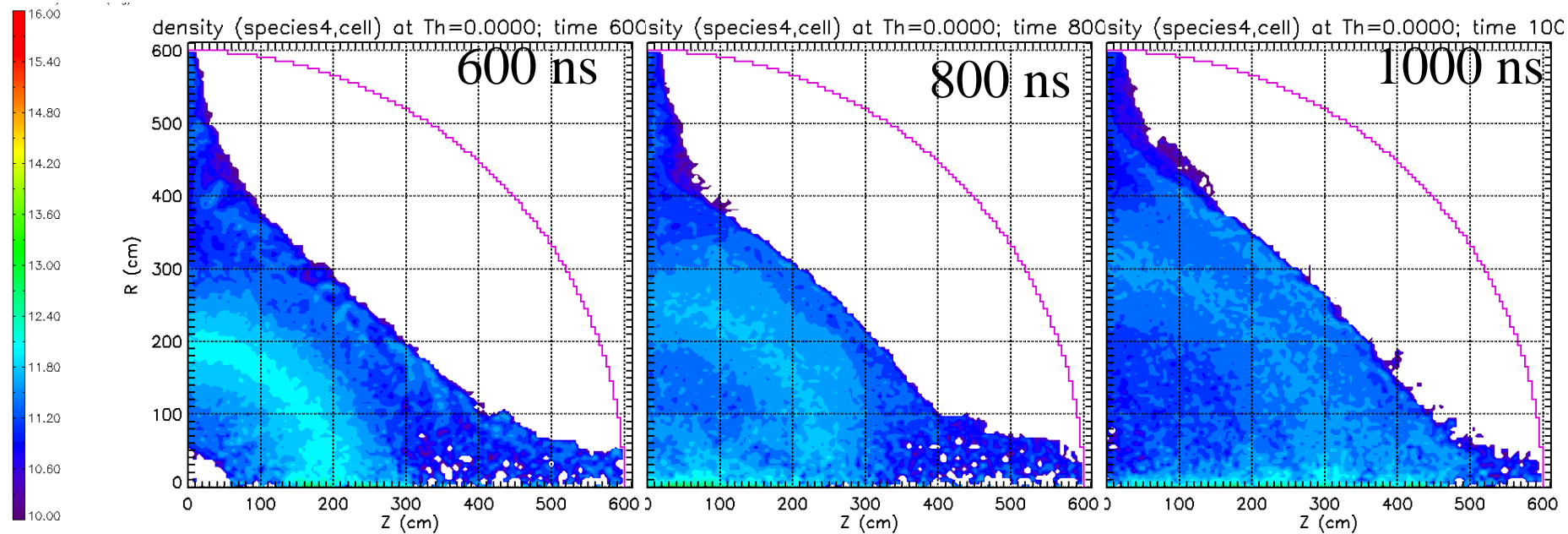
- A preliminary simulation result using the new solver and 5 species from the Perkins ion spectra is given (H, D, T,  $^4\text{He}$ ,  $^{12}\text{C}$ ).
- For computational expediency, ion distributions all truncated at  $v_i=0.1c$ .
- 4-coil magnetic field topology taken from previous “shell” model calculations of Robson and Genoni.

# Computational constraints are significant for these ion speeds and scale lengths:

---

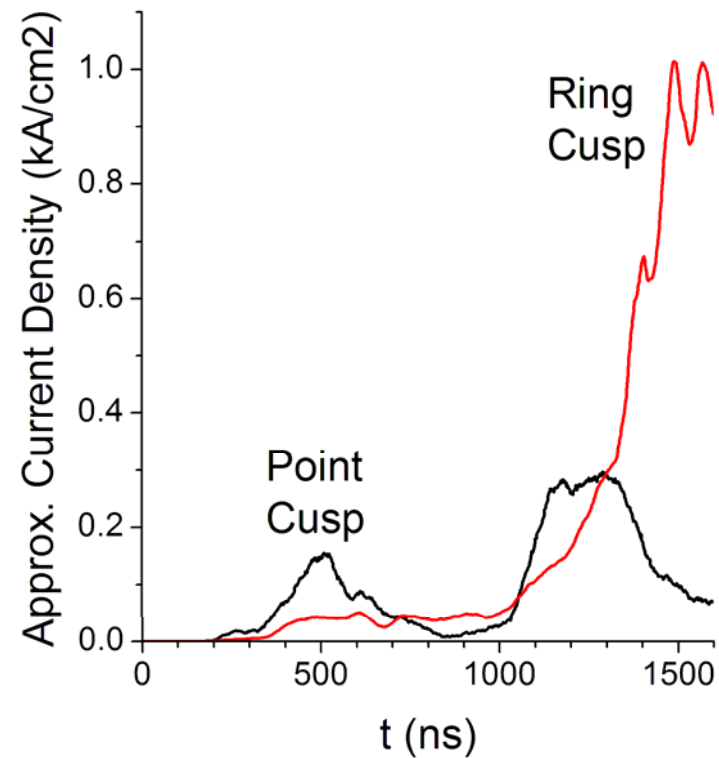
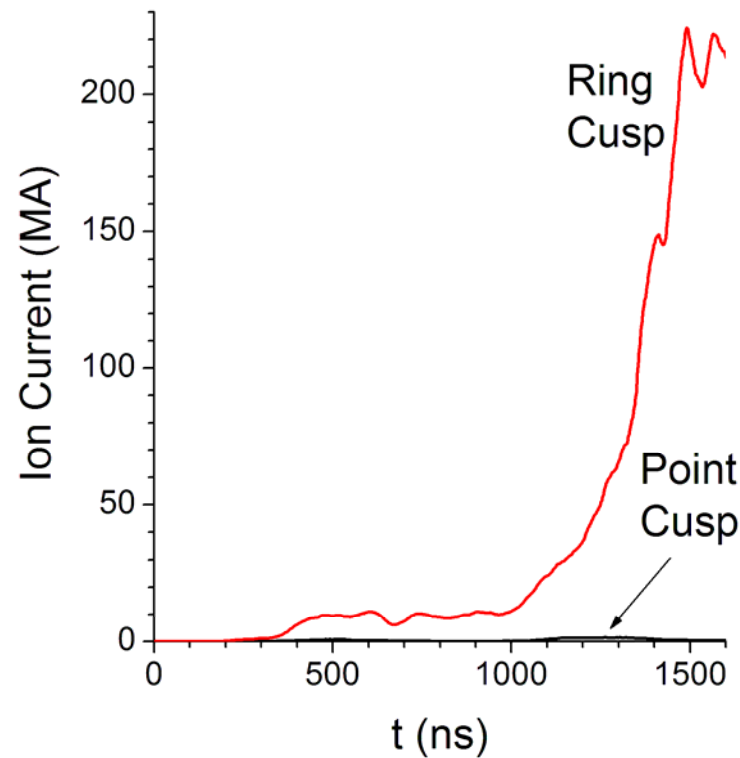






# Ion current densities at point and rings cusps are less than $\sim 1$ kA/cm (so far!)

---



# Status: Magnetic Intervention Chamber Modeling

---

- A representative “shell” simulations are consistent with “shell” models of Robson and Genoni.
- Problems with the convergence of the solver (as seen in the Pechacek simulations) need to be resolved.
- Unlike the Pechacek experiment, the magnetic intervention parameter regime ion speeds and scale lengths may require *significant* computational resources using the EMHD algorithm. A parallel implementation of this algorithm is essential.

## 5: Next Steps...

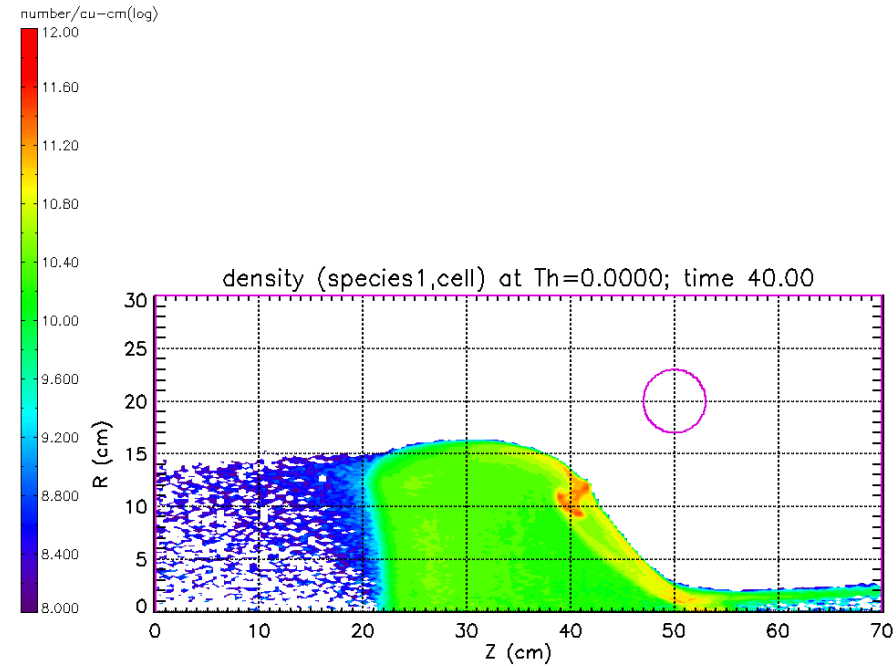
- Continue to refine EMHD solver...
  - Non-uniform grids
  - Parallel implementation
- Complete analysis of Pechacek experiment and document
- Continue examination of magnetic intervention physics issues
  - Shock acceleration of ions at sheath...
  - Currently revisiting perfectly conducting “shell” model formulation for use on a fixed grid with arbitrary number of particles.



# Extra slides

EMHD simulation used  $\sim 15,600$  particles (protons)  
Explicit PIC simulation used  $\sim 2,000,000$  particles  
(1,700,000 electrons, 300,000 protons)

Gamble II MI expt.,  $B=1.6\text{kG}$ , 20 deg, mono-energetic: gamble.lsp - Wed Mar 15 14:11:33 20



# Experimental Parameters

- Chamber wall radius is 30 cm (not shown)
- External field coils, 67 or 70 cm diam, 70 cm separation.
- $|B| = 2.0$  kG at ring cusp.
- $2 \times 10^{19}$  “D<sub>2</sub>” ions produced from cylindrical target of 1-mm diam., 1-mm length.
- Modeling assumes initial plasma is a thermal (51.1 eV), D<sup>+</sup> neutral plasma with initial radius of 2 cm.

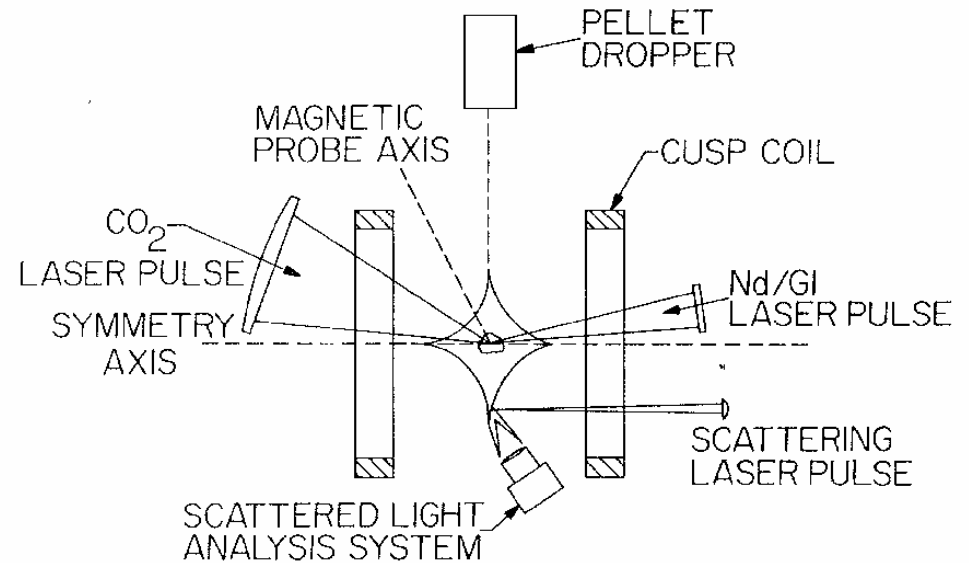


FIG. 1. Schematic diagram of the cusp experiment. The coil diameter is 70 cm. The scattered-light analyzing system and the incident-scattering laser pulse are actually in the same horizontal plane.

# Plasma/Field boundary along 27 degree radial line from the cusp center (experimental result):

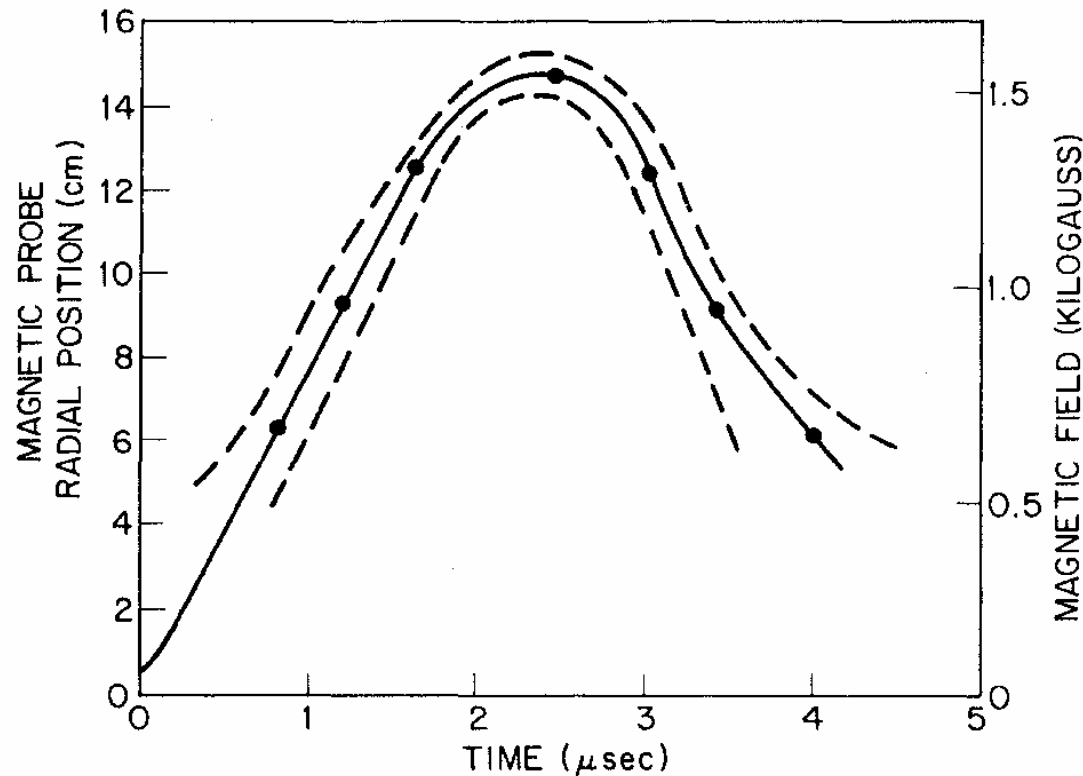


FIG. 3. Radial position of the plasma-magnetic-field interface vs time after the peak of the  $\text{CO}_2$  laser pulse, derived from the time of arrival of the peak of the diamagnetic signal from a probe that is movable along a radial line inclined at  $27^\circ$  to the midplane. The dashed curves represent the half-peak points of the  $\dot{B}$  signal.

At  $r=22$  cm inside ring cusp, electron density was measured at 5 different times:

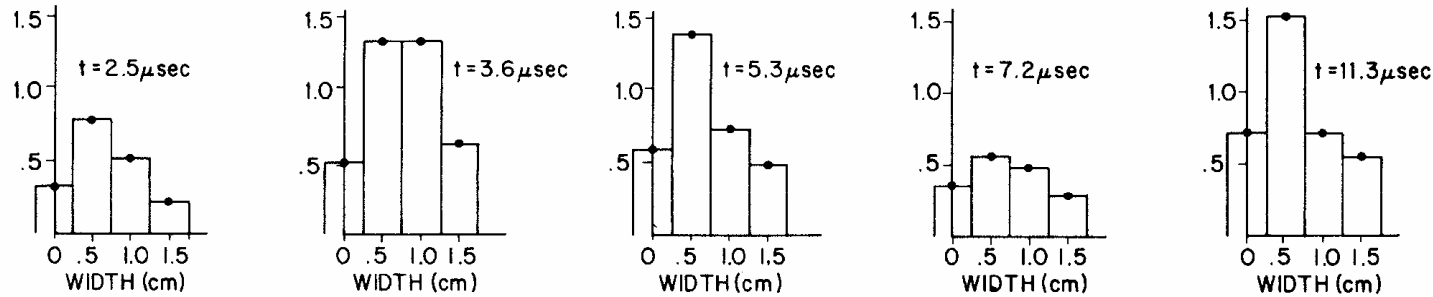
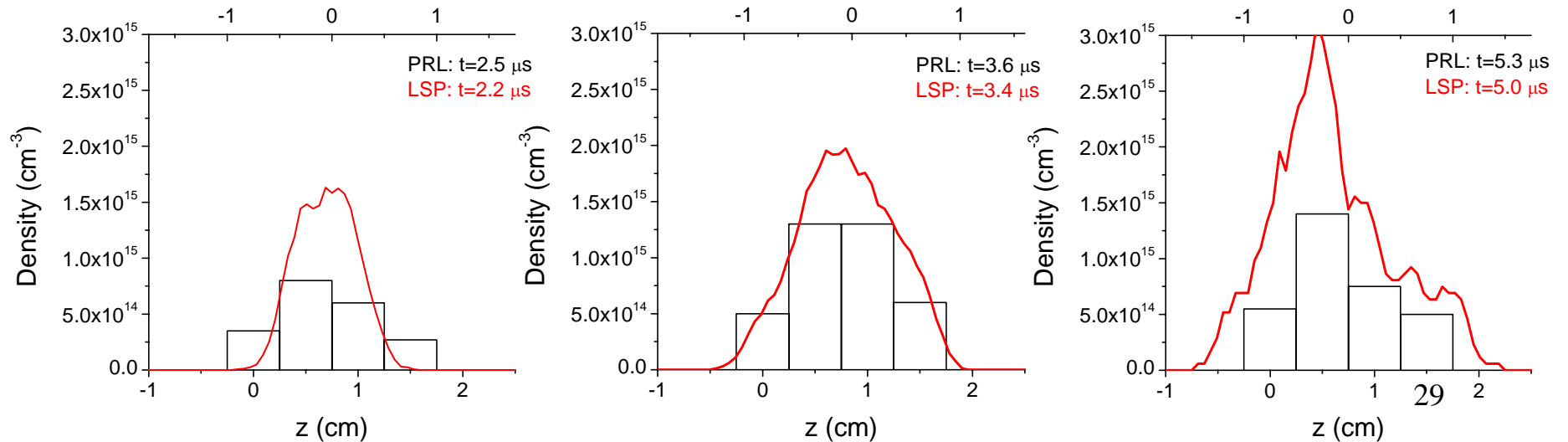


FIG. 4. Electron density as a function of position across the width of the ring cusp, at time  $t$  after the creation of the plasma. Each point is an average of two to four shots. The units of the vertical axes are  $10^{15} \text{ cm}^{-3}$ .

Simulations results in reasonable agreement with these measurements (at least for first 3 times):



Simulation dynamics are complex, but energy gain in all species (except protons?) is consistent with diffusion of plasma into sheath.

